ФИЗИКА ЭЛЕМЕНТАРНЫХ ЧАСТИЦ И АТОМНОГО ЯДРА
2004. Т. 35. ВЫП. 2

УДК 539.172.4; 621.039.78

NEUTRON SPECTROSCOPY INVESTIGATIONS WITH GELINA

H. Weigmann

European Commission, Joint Research Centre,
Institute for Reference Materials and Measurements, Geel, Belgium

INTRODUCTION 519
THE GELINA TIME-OF-FLIGHT FACILITY 520
DATA FOR APPLICATIONS 522
PHYSICS ASPECTS 528
REFERENCES 532

ФИЗИКА ЭЛЕМЕНТАРНЫХ ЧАСТИЦ И АТОМНОГО ЯДРА
2004. Т. 35. ВЫП. 2

УДК 539.172.4; 621.039.78

NEUTRON SPECTROSCOPY INVESTIGATIONS WITH GELINA

H. Weigmann

European Commission, Joint Research Centre,
Institute for Reference Materials and Measurements, Geel, Belgium

The Geel Linear Accelerator (GELINA) is a 150 MeV electron linac which together with a pulse compression system and a Hg cooled U target is operated as a pulsed white neutron source for the measurement of neutron induced nuclear interaction data in the neutron energy range from below thermal to about 20 MeV. After a short description of the major parameters of the facility, some of the experimental work performed at GELINA during the past years is described. Emphasis is put on the excellent neutron energy resolution achieved by a 1 ns electron burst width and neutron flight paths of up to 400 m length. The major part of the research programme concerns the measurement of data required for applications in reactor calculations, for feasibility studies of advanced reactor concepts and waste transmutation scenarios including accelerator driven systems, and for the safety assessment of such systems and the nuclear fuel cycle. Some of the work simultaneously delivers interesting information on nuclear structure at several MeV excitation energy.

Линейный ускоритель GELINA в Геле (Бельгия) является электронным ускорителем на энергию 150 МэВ, который вместе с системой временного сжатия импульса и урановой мишенью, охлаждаемой ртутью, работает как импульсный источник нейтронов белого спектра для получения данных о взаимодействии с ядрами нейтронов с энергиями от ниже тепловых до $\sim$ 20 МэВ. После краткого описания основных параметров установки приводится обзор нескольких экспериментальных работ, проведенных на GELINA в последние годы. Особенно подчеркивается превосходное разрешение по энергии нейтронов, достигаемое при ширине электронной вспышки 1 нс для нейтронных пролетных баз длиной до 400 м. Основную часть исследовательской программы составляли измерения данных, используемых для расчетов реакторов, для изучения возможности развития реакторных технологий и сценариев выжигания (трансмутации) радиоактивных отходов, включая системы, управляемые ускорителем, и для оценки безопасности таких систем и ядерных топливных циклов. В то же время некоторые из рассматриваемых работ содержат интересную информацию о структуре ядер при энергиях возбуждения порядка нескольких МэВ.

INTRODUCTION

The measurement of cross sections and related parameters for neutron induced nuclear reactions with high energy resolution is of interest both for applications related to nuclear energy and for basic nuclear physics research.

The importance of neutron cross section data for the design and the safety assessment of nuclear energy systems and the fuel cycle needs no further explanation. High resolution data are especially important for applications in shielding

calculations, where the rapid fluctuations in the cross sections produce a significant difference as compared to an assumed smooth cross section, and for applications, where the resonance structure of the cross sections is relevant as is the case for the assessment of self-shielding and the reactor temperature coefficient of reactivity.

The interest of high resolution neutron cross section data for basic nuclear physics lies, dependent on the nucleus under consideration, in the exploitation of the statistical properties of nuclei — including deviations from the usual statistical behaviour — and in the study of nuclear structure at several MeV excitation energy.

During decades of work, several laboratories in the world have produced a rich amount of neutron nuclear reaction data. These data have been compiled by nuclear data centres co-operating in a world-wide network. High resolution cross section data are generally being measured by the time-of-flight method. The best energy resolution is available at the ORELA facility of Oak Ridge National Laboratory, the LANSCE facility of Los Alamos National Laboratory, and the GELINA facility of the Institute for Reference Materials and Measurements (IRMM) of the Joint Research Centre of the European Union at Geel, Belgium. Recently, an additional facility called n-TOF, has been set up at CERN, Switzerland, with the special goal of measuring cross sections needed for feasibility studies of accelerator driven nuclear energy systems.

In the present paper a review will be given of high resolution neutron data measurements performed at the GELINA facility of IRMM. In Sec. 1 a very short description of the facility will be given. Section 2 will deal with measurements performed for various applications, e. g., in nuclear energy and its safety and the nuclear fuel cycle. In Sec. 3 some more basic physics studies will be described, and in Sec. 4 an outlook into the near future will be tried.

1. THE GELINA TIME-OF-FLIGHT FACILITY

GELINA [1] is a 150 MeV electron linac which, together with a pulse compression magnet and its neutron producing targets, serves as a pulsed white neutron source for a multiple neutron time-of-flight spectrometer.

The injector of the accelerator consists of a triode gun followed by a prebunching cavity, a 10 cm drift space, and a standing wave buncher. Currents of up to 15 A may be injected into the buncher. The system delivers electron pulses from 4 ns (FWHM) to 2 μs, adjustable in discrete steps for a pulse duration between 4 and 50 ns, or in a continuous way between 40 ns and 2 μs. The maximum pulse repetition rate is 1 kHz for 4–100 ns pulses, and 250 Hz for 2 μs pulses. The standing-wave buncher is followed by two 6 m long travelling-wave sections which can accept up to 35 MW peak rf power (50 kW average) and are operated at 3 GHz (S-band).

A post-acceleration pulse compression system [2] to reduce the pulse length of the electron burst is installed at the exit of the accelerator. The working principle is the following: The electron burst (typically 10 ns) consists of about 30 microbunches of 10–20 ps length, spaced at intervals of 333 ps corresponding to the 3 GHz of the accelerator operation. As the filling time of the sections is 1.1 μs, the electrons gain their energy only from the electromagnetic energy stored in the cavities. When accelerated along the sections, each of the microbunches uses a part of this stored energy, and therefore the energy of the bunches decreases stepwise from one bunch to the next. The train of microbunches is then injected into a large magnet designed in such a way that the beam leaves the magnet in the original direction after a full turn. The first microbunch in the pulse, having the highest energy, travels the longest path inside the magnet. Conversely, the last microbunch, having the lowest energy, exits the magnet much faster. Therefore, the time-correlated decrease of electron energies is transformed into a time-correlated decrease of trajectory lengths. With appropriate dimension of the magnet, injecting pulses of 10 ns length and 10 A, one obtains routinely, at the output of the magnet, pulses of the order of 1 ns duration and up to 100 A peak current.

After compression, the electron beam impinges upon a rotary uranium target that can dissipate more than 12 kW, the maximum average beam power available. It consists of a torus of depleted uranium-10 % molybdenum, cladded with stainless steel and cooled by a flow of mercury. The target rotates slowly in order to distribute the heating power over a larger volume. It is mounted on a lift for remote-controlled storage in an underground bunker. Fast neutrons are produced in the uranium by (γ, n) and (γ, f) reactions. Two moderators made of water filled beryllium boxes are placed below and above the uranium target

Main characteristics of the GELINA facility

Pulse length, ns	Repetition rate, Hz	Peak current, A	Mean current, μA	Average energy, MeV	Mean power, kW	Neutron rate in pulse, n/s	Mean neutron rate, n/s
Without compression							
5	800	12	48	110	5.3	$6.4 \cdot 10^{18}$	$2.5 \cdot 10^{13}$
10	800	12	96	100	9.6	$5.6 \cdot 10^{18}$	$4.4 \cdot 10^{13}$
100	800	1.50	120	87	10.4	$0.6 \cdot 10^{18}$	$4.8 \cdot 10^{13}$
1000	380	0.22	83	100	8.3	$0.1 \cdot 10^{18}$	$3.8 \cdot 10^{13}$
2000	250	0.22	110	100	11	$0.1 \cdot 10^{18}$	$5.0 \cdot 10^{13}$
With compression							
< 1	800	~ 100	75	100	7.5	$4.6 \cdot 10^{19}$	$3.4 \cdot 10^{13}$

for the production of an intense flux of low energy neutrons which exhibit an approximate $1/E$ spectrum. The table summarizes the main characteristics of the facility.

The compression magnet and the target-moderator system are installed in a bunker with 3 m thick concrete walls. Several neutron flight paths of 25–50 cm diameter, radially positioned around the target, leave the bunker and extend to a length which varies between 7 and 400 m. Collimation at the entrance to the flight paths can be arranged such that in an experiment one may use either the high-energy neutrons emitted directly from the uranium target or the low energy neutrons emitted from the water moderators. Up to twelve experiments can be carried out simultaneously.

2. DATA FOR APPLICATIONS

The experimental programme at GELINA follows the recommendations of the OECD-NEA Nuclear Science Committee as summarized in its «High Priority Nuclear Data Request List» [3] which includes demands for accurate measurements of neutron data for fission reactor technology, fission reactor and fuel cycle safety, waste transmutation, and fusion reactor blanket calculations.

The amount of data needed for these applications and to be included in evaluated data libraries, is much too large to be obtained by measurements. On the other hand, recent progress in nuclear model calculations [4, 5] is such that

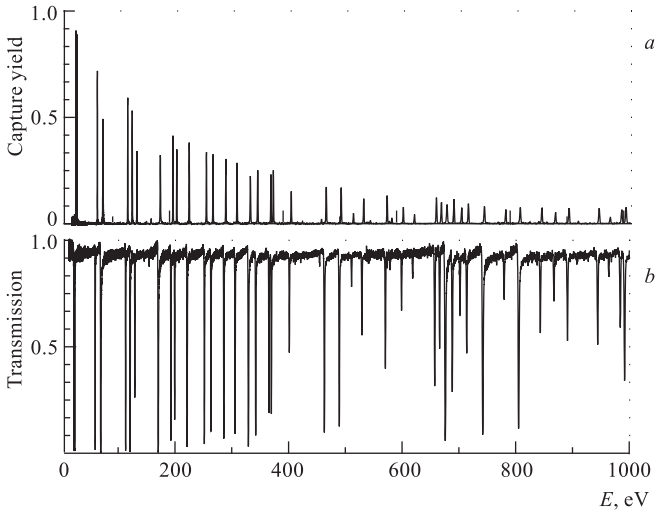

Fig. 1. Capture yield (*a*) and transmission (*b*) of ^{232}Th measured at GELINA

many of the data which are not demanded with high accuracy, can be obtained by model calculations, provided that good input data are available for these calculations. Therefore, in the experimental programme increased emphasis is put on providing the input data required for model calculations, such as optical model parameters, level densities, strength functions, resonance partial widths. Especially in heavy nuclei with a large level density, high resolution measurements of resolved resonance properties up to energies as high as possible are important.

Measurements on the more common fissile and fertile isotopes have been done for many years, and the status of data libraries is rather satisfactory. More recently, measurements are being performed which are needed for the feasibility study of waste transmutation scenarios, i. e., measurements on minor actinides and long-lived fission products. Examples for the latter are measurements at GELINA on ^{99}Tc [6] and ^{129}I [7]. Also, the Th fuel cycle, which had received little attention in the past, has recently gained increased interest. Therefore, new measurements of the total and capture cross sections are being performed at GELINA [8]. Figure 1 shows part of the measured raw data in the resonance region.

As mentioned above, one of the more important parameters needed for model calculations is the nuclear level density. Measurements of resolved resonances offer the most direct means to determine the level density, in principle simply by counting the number of observed resonances. However, care must be taken when interpreting the observed data: at low neutron energies, essentially only s-wave resonances are being observed, but small ones may be missed, or large p-wave resonances may be admixed in the observed set. To correct for such effects, use may be made of the statistical distribution of the resonance neutron widths. Figure 2 shows an example for the case of ^{240}Pu. The integral distribution of reduced neutron widths of the observed resonances (i. e., the number of resonances which have a reduced width larger than the value given on the abscissa) is compared to the expected Porter–Thomas distribution which has been fitted to the observed

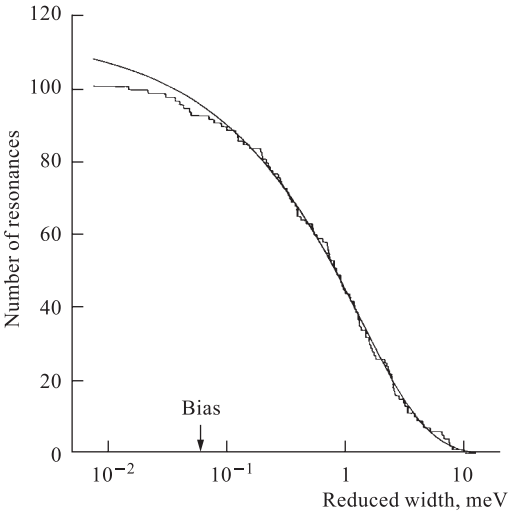

Fig. 2. Comparison of the observed resonance neutron widths for ^{240}Pu to a Porter–Thomas distribution fitted to the data above the indicated bias. The deviation for small widths is due to the resonances missed in the experiment

data above the indicated bias. The deviation for small widths is due to the resonances missed in the experiment. Level densities extracted from measured resolved resonance data should be trusted only if such or a similar correction has been performed.

Of special concern for reactor applications is the resonance Doppler broadening, as it constitutes a major contribution to the temperature coefficient of reactivity. Usually, in reactor codes the Doppler broadening is calculated using the ideal gas approximation. In order to determine the deficiencies of this approximation and to eventually arrive at a more realistic description, in the frame of an international collaboration (besides IRMM: CEA, ILL Grenoble, TU Delft, University of Kiel) the Doppler broadening of low energy neutron resonances has been investigated. Transmission measurements have been performed for several samples (U, UO_2, NpO_2, Hg_2Cl_2) at temperatures between 24 and 293 K [9]. As an example, Fig. 3 shows results for NpO_2: a comparison of the measured transmission in the region of the 3.85 eV resonance in ^{237}Np with calculated resonance

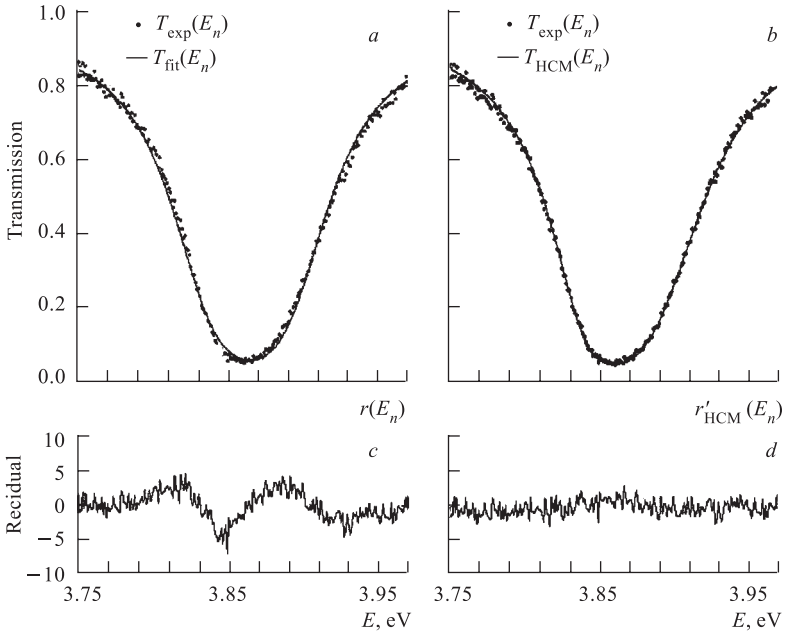

Fig. 3. Doppler broadening of the 3.85 eV resonance of ^{237}Np in NpO_2 at $T = 50$ K. Comparison between the experimental transmission and the calculated one using the ideal gas approximation (*a*, *c*) and the condensed matter Doppler routine DOPUSH (*b*, *d*), from Ref. 9

shapes using the gas approximation (Fig. 3, *a*, *c*) and the condensed matter routine DOPUSH [9] (Fig. 3, *b*, *d*).

In lighter nuclei with a lower level density, resolved resonances are observed up to the hundreds of keV or the MeV regions. As an example, Fig. 4 shows a small part (from 615 to 650 keV neutron energy) of the measured [10] total cross section of ^{60}Ni. The figure illustrates the high resolution still achieved in the hundred's of keV region, and it also demonstrates why high resolution is important for certain applications, especially for shielding: the cross sections show a pronounced structure, with very deep minima due to interference of resonance- and potential scattering, where the cross section goes to almost zero. In fact, for shielding applications an accurate knowledge of these minima is more important than of the average cross section. From Fig. 4 it can also be seen that, as long as elastic scattering is the main contribution to the total cross section, with sufficient energy resolution the spins of many resonances can directly be read from the resonance shapes and the peak total cross section. The drawn line in Fig. 4 represents an R-matrix fit to the data.

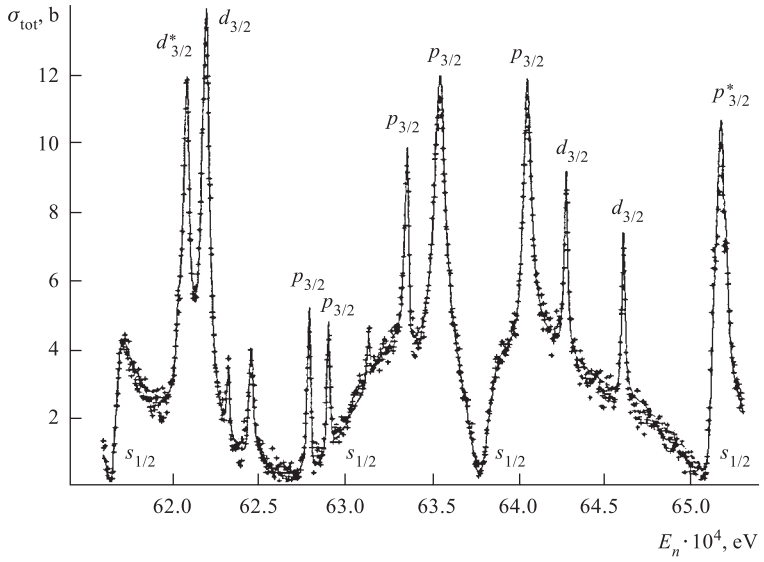

Fig. 4. Measured total cross section of ^{60}Ni and *R*-matrix fit [10]

In the MeV region for structural materials nuclei such as Fe, Cr, and Ni resonances are no longer resolved, but structure still prevails, and it is important for applications such as shielding. In Fig. 5, *a* part of the measured total cross

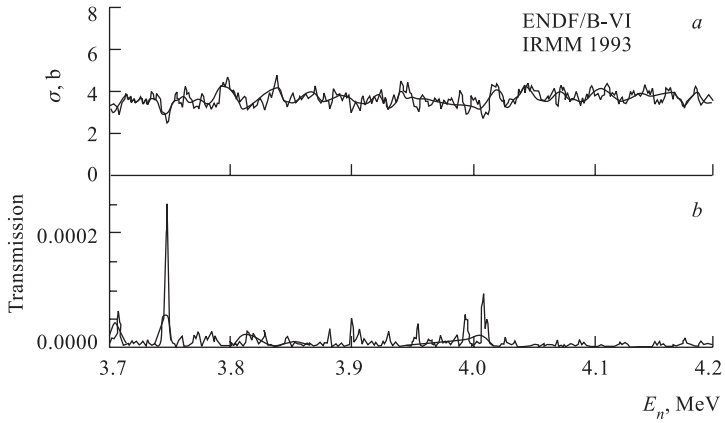

Fig. 5. *a*) Measured total cross section of Fe compared to ENDF/B-VI; *b*) corresponding transmission through 40 cm of Fe [11]

section of Fe [11] is shown. The figure illustrates the amount of structure still present in the MeV region. In comparison to the measured cross section also the ENDF/B-VI data file (more smooth curve) is indicated in the figure. That the measured larger fluctuations may still be important is demonstrated in Fig. 5, *b*: it shows the transmission through 40 cm of Fe as calculated from the two cross section sets. One observes that where the fluctuating cross section has minima, the corresponding transmission shows sharp peaks. As a consequence, although the two average cross sections are identical, the average transmissions differ by 25 %.

The use of high resolution total cross sections such as the one of Fig. 5 in applications first met a problem: Processing routines for reactor calculations do not allow the use of fluctuating total cross sections together with smooth partials. Therefore, the fluctuations observed in the total cross sections were numerically imposed also on all partials. However, this is unphysical: Resonance partial widths for elastic and inelastic channels have different angular momentum dependences and, more important, are supposed to independently fluctuate according to Porter–Thomas distributions. Thus, fluctuations in the total and partial cross sections are at best weakly correlated. Therefore, existing high resolution total cross section data had to be complemented by the measurement of inelastic scattering cross sections with similar energy resolution. Such measurements have been performed on several isotopes, besides ^{56}Fe also Al and Na. In order to achieve the required high resolution, time-of-flight techniques have been used with flight paths between 60 and 200 m, and the γ rays emitted after inelastic scattering are detected in fast scintillation detectors.

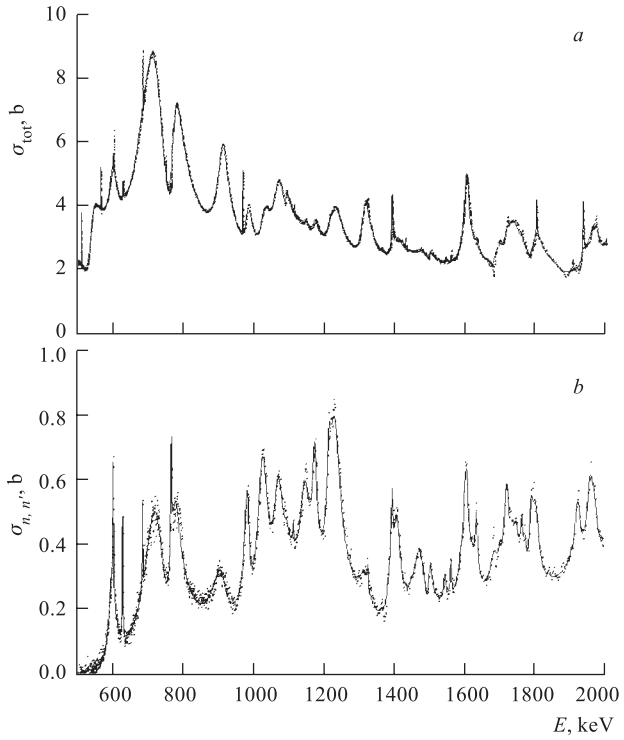

Fig. 6. Total cross section (*a*) and inelastic scattering cross section (*b*) of Na; the dots are the measured data, the smooth curve is an R-matrix fit by the code SAMMY [14]

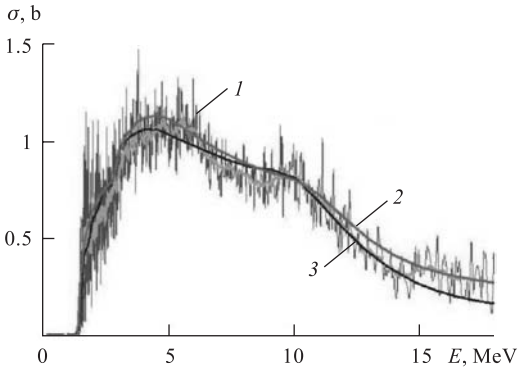

Fig. 7. The inelastic scattering cross section of ^{58}Ni [15]: *1* — this work; *2* — this work after smooth; *3* — Stapre

As an example the measured [12] inelastic scattering cross section from the lowest level of Na at about 400 keV is shown in Fig. 6, *b*. Figure 6, *a* shows the total cross section as measured at ORELA [13]. The dots are the measured data, while the smooth curve shows an R-matrix fit [12] to the data obtained with the code SAMMY [14].

More recently, similar work has been carried out on Cr and Ni isotopes [15]. In these measurements the scintillation detectors have been replaced by HP Ge detectors in order to achieve a better separation of γ-ray lines and thereby also a better background discrimination. As an example, Fig. 7 presents results obtained for ^{58}Ni. The figure shows the inelastic scattering cross section as deduced from the measured γ-ray production cross sections (above 5.6 MeV neutron energy there is a slight uncertainty due to incomplete knowledge of the ^{58}Ni decay scheme) together with some model calculations (smooth curves). For more details and references to the earlier work see Ref. 15.

3. PHYSICS ASPECTS

In a typical heavy nucleus, individual resonances may be resolved up to several keV neutron energy, and a few hundred s-wave resonances (spin $1/2^+$) may be observed within this energy range. No detailed information on the structure of these resonance states (e. g., in terms of shell-model configurations) will be obtainable because of two reasons: First of all, with the resonance density exceeding the density of single particle states by more than 4 orders of magnitude, the internal structure of these states will be too much complicated to be understood theoretically, and furthermore the energy range of a few keV available to experiment is too small for a meaningful investigation of nuclear structure properties.

On the other hand, the large number of levels observed for a given spin state, provides a valid basis for studies of their statistical properties — and of deviations from the statistical expectation indicating «doorway» mechanisms or other structure effects, and such studies have indeed been a prominent objective of neutron resonance spectroscopy for many years. The statistical quantities of interest are:

• The nuclear level density, its dependence on excitation energy, spin and parity. The level density is not only important for practical applications in nuclear models, it also reveals basic information on, e. g., shell structure and on the interplay between single particle and collective modes of excitation.

• Strength functions or average partial widths and their energy dependence. Neutron strength functions in nuclei with a sufficiently large level density are expected to be fairly energy independent as possible structures due to simple configurations like $2p{-}1h$ or particle+vibration states which may in principle

be present, will be washed out when their spreading widths will exceed their spacings. Nevertheless, significant variations of neutron strength functions over energy ranges of the order of 10 eV to a few 100 eV have been observed for several nuclei. One distinct example occurs in ^{98}Mo where a group of p-wave resonances with very large reduced neutron widths is found in the energy range from 400 to 850 eV. The probability for accidental occurrence of this peak in the strength function due to Porter–Thomas fluctuations is smaller than 7 % [15]. It is hard to imagine how any particular configuration having a large neutron width would have a spreading width of only ≈ 500 eV in a nucleus with a fairly large level density, and no satisfactory explanation has been put forward. Nevertheless, the possible occurrence of such narrow structures may cast some doubt on the commonly assumed statistical properties of resonances.

• The statistical distribution of partial widths as well as possible correlations between partial widths related to different reaction channels. The latter are in fact a signature of deviations from the statistical situation related to structure effects like doorways states or pre-equilibrium emission. One of the most distinct examples are again the strong p-wave resonances in ^{98}Mo mentioned above, where the two resonances at 429 and 612 eV exhibit an almost identical γ-decay spectrum, and the partial radiative widths are essentially proportional to the reduced neutron widths of the resonances. Such effects are attributed to the existence of a common (to the channels in question) doorway state, which in the case of (n, γ) reactions is interpreted in terms of the so-called valence model [16, 17].

• Another clear signature of a doorway state mechanism is of course the well-known intermediate structure in resonance region fission cross sections. Here one is dealing with an interesting combination of nuclear structure aspects (the potential energy as a function of deformation) and statistical properties of the individual states in the two potential wells and their interaction.

The situation is different in nuclei with a low level density, i. e., light nuclei ($A < 40$) and nuclei around doubly closed shells like the Pb region. «Resolved» resonances may be observed up to a few MeV neutron energy, thus over a sufficiently broad range of excitation energies, and they may be expected to be sufficiently simple in structure that one may attempt to reproduce their properties, especially reduced neutron widths, in terms of model calculations. Below, two cases will be discussed where measurements at GELINA have contributed to the understanding of the physical situation: resonances in $^{28}\mathrm{Si} + n$ [18], and $^{207}\mathrm{Pb} + n$ [19].

Figure 8 shows a small part (from 1.15 to 1.28 MeV neutron energy) of the measured total cross section of ^{28}Si together with an R-matrix fit to the data. The figure demonstrates a good energy resolution as well as the quality of the R-matrix fit. The R-matrix analysis yields the resonance neutron widths and it also allows one to identify most of the resonance spins, but many resonance spins

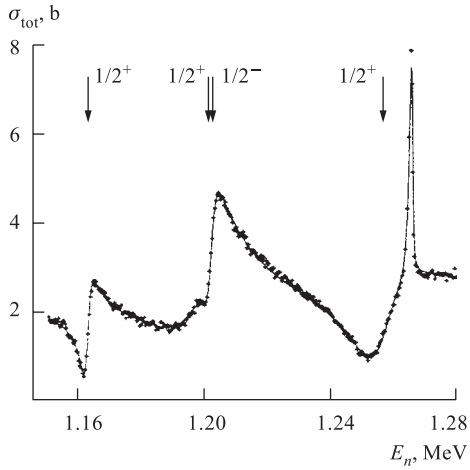

Fig. 8. The measured total cross section of ^{28}Si and R-matrix fit

have also been determined from measurements of the capture γ rays leading to the ground- and first excited states of ^{29}Si, including their angular distributions.

In Fig. 9 the experimental results are compared to model calculations of Halderson et al. [20]. The cumulative sum of reduced neutron widths is plotted as a function of neutron energy, separately for spins $1/2^+$, $1/2^-$, and $3/2^-$. The general picture is that such model calculations underpredict the number of resonances observed, but they reasonably well predict the total strength in the investigated energy interval of 3 MeV.

The $1/2^+$ resonance at 1.201 MeV marked in Fig. 8 is of special interest: it is identified with the isobaric analogue to the first excited state in ^{29}Al, the position of which at this excitation energy was known from $^{30}\mathrm{Si}(^3\mathrm{He}, \alpha)$ measurement of Detraz and Richter [21]. The observation of this state as a resonance in a neutron cross section has two interesting aspects:

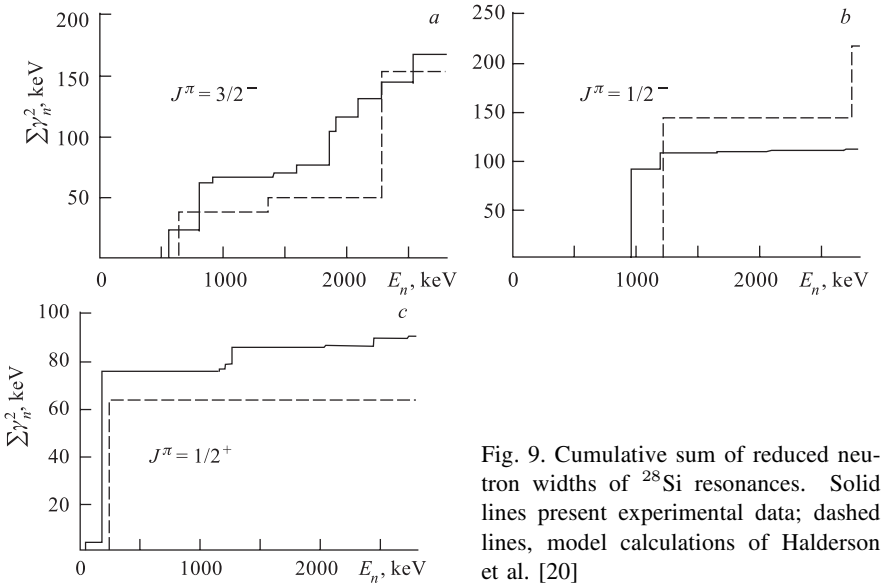

Fig. 9. Cumulative sum of reduced neutron widths of ^{28}Si resonances. Solid lines present experimental data; dashed lines, model calculations of Halderson et al. [20]

• The high accuracy of the energy determination allows a precise check of the isobaric multiplet mass equation.

• Since the excitation of a $T_>$ state in a neutron induced reaction is isospin forbidden, its neutron width as obtained from the total cross section is a direct measure of its isospin impurity.

Similar isobaric analogue resonances with no isospin allowed decay channel have been observed in other neutron induced reactions on $N = Z$ nuclei like $^{24}\mathrm{Mg} + n$ [22] and $^{32}\mathrm{S} + n$ [23].

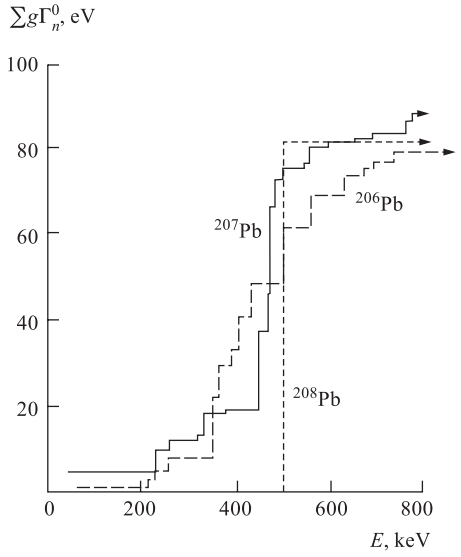

Fig. 10. Doorway states in Pb isotopes

Similar to the case of ^{28}Si, also in $^{207}\mathrm{Pb}+n$ [19] measurements were performed of the total cross section and the partial capture cross sections leading to the ground and first excited states of ^{208}Pb, and again resonance spins were determined with the help of an R-matrix fit to the total cross section and on the basis of the observation of the partial γ rays and their angular distributions. Part of the results obtained are presented in Fig. 10. The figure shows the cumulative sum of reduced neutron widths of s-wave resonances together with corresponding resonances in $^{208}\mathrm{Pb} + n$ [24] and $^{206}\mathrm{Pb} + n$ [25]:

In ^{208}Pb with its double shell closure there is a single very strong s-wave resonance at about 500 keV neutron energy which certainly is due to a simple

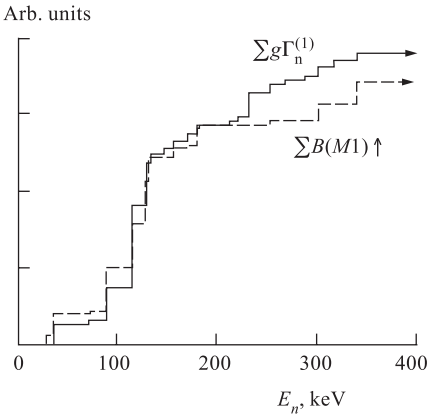

Fig. 11. Comparison of cumulative sums of reduced neutron widths and magnetic dipole strengths for ground state transitions from 1^+ resonances in $^{207}\mathrm{Pb} + n$

configuration (the large shell gap does not allow for multiple excitations at comparatively low energies). In the neighboring isotopes, the additional quasiparticles allow additional excitations which result in a much larger level density. As a consequence, the one strong resonance of ^{208}Pb is now fragmented into a dozen of resonances which however share the same total strength in the form of a typical S-shaped doorway structure.

The measurements on $^{207}\mathrm{Pb} + n$ were primarily performed in order to study the fragmented giant magnetic dipole resonance in ^{208}Pb by the observation of ground state transitions from 1^+ resonances. A total of 33 resonances could definitely be assigned spin 1^+, and the magnetic dipole strengths of the resonances below 400 keV neutron energy are plotted in Fig. 11 together with the reduced neutron widths. The arbitrary vertical scales are chosen to show the similarity of the two patterns. The plot exhibits the signature of a common (to the neutron and ground state capture channels) doorway state.

CONCLUSION

The GELINA facility is one of the most powerful pulsed neutron sources for neutron nuclear data measurements worldwide. It provides excellent possibilities for the measurement of cross sections and related parameters for neutron induced nuclear reactions over a wide energy range (about 10 meV to 10 MeV). Its particular strength is the excellent neutron energy resolution achieved by the combination of a 1 ns accelerator burst width and flight paths up to 400 m length. This feature is of special importance for measurements in the hundreds of keV and in the MeV region where marked structures still exist in the cross sections of many nuclei, and an adequate knowledge of these fluctuations is needed for neutron transport calculations and shielding applications. The excellent energy resolution is also important for the identification and characterization of compound nuclear resonances — in nuclei with a high level density for the study of their statistical properties, in nuclei with a sufficiently small level density for the investigation of nuclear structure at several MeV excitation energy.

Acknowledgements. The author wishes to thank P. Rullhusen, A. Plompen, and P. Siegler for useful discussions and a critical reading of the manuscript. Thanks are especially due to A. Plompen, A. Brusegan, and P. Schillebeeckx for communicating results prior to publication.

REFERENCES

1. *Bensussan A., Salome J-M.* // Nucl. Instr. Meth. 1978. V. 155. P. 11.
2. *Tronc D., Salome J-M., Bockhoff K. H.* // Nucl. Instr. Meth. 1985. V. 228. P. 217.
3. Report NEA/NSC/DOC(97)4, OECD-NEA. 1997.

4. *Avrigeanu M., Avrigeanu V.* STAPRE-H95 Computer Code, IPNE Report NP-86-1995. Bucharest 1995; News NEA Data Bank. 1995. V. 17. P. 22; 25.

5. *Koning A. J., Hilaire S.* TALYS, a Computer Code System for the Simulation and Analysis of Nuclear Reactions. To be published.

6. *Gunsing F. et al.* // Proc. of the Intern. Conf. on Nuclear Data for Science and Technology, Trieste, 1997. Bologna, 1997. P. 1293;
Raepsaet C. et al. // Ibid. P. 1289.

7. *Noguere G. et al.* // Proc. of the Intern. Conf. on Nuclear Data for Science and Technology, Tsukuba, 2001. Nucl. Sci. and Techn. Suppl. 2. 2002. P. 184.

8. *Volev K. et al.* // Proc. of the Intern. Workshop on P&T and PDS Development, Mol, Belgium, Oct. 6–8, 2003. To be published.

9. *Gressier V., Nabarejnev S., Mounier C.* // Ann. Nucl. Energy. 2000. V. 27. P. 1115.

10. *Brusegan A. et al.* // Proc. of the Intern. Conf. on Nuclear Data for Science and Technology, Gatlinburg, 1994; ANS, Ill. 1994. P. 224.

11. *Berthold K. et al.* // Ibid. P. 218.

12. *Kopecky S. et al.* // Proc. of the Intern. Conf. on Nuclear Data for Science and Technology, Trieste, 1997; Bologna, 1997. P. 523.

13. *Larson D. C.* EXFOR-10761.002. 1978.

14. *Larson N. M.* ORNL-Report ORNL/TM-9179/R3. 1996.

15. *Plompen A. J. M. et al.* Physor 2002; Proc. of the Intern. Conf. on the New Frontiers of Nuclear Technology: Reactor Physics, Safety and High-Performance Computing. Korean Nucl. Soc.; Am. Nucl. Soc., 2002.

16. *Rohr G., Weigmann H., Winter J.* // Nucl. Phys. A. 1970. V. 150. P. 97.

17. *Chrien R. E. et al.* // Phys. Rev. C. 1976. V. 13. P. 578.

18. *Weigmann H. et al.* // Phys. Rev. C. 1987. V. 36. P. 585.

19. *Kohler R. et al.* // Ibid. V. 35. P. 1646.

20. *Halderson D. et al.* // Ann. Phys. (N.Y.). 1977. V. 103. P. 133.

21. *Detraz C., Richter R.* // Nucl. Phys. A. 1970. V. 158. P. 393.

22. *Weigmann H., Macklin R. L., Harvey J. A.* // Phys. Rev. C. 1976. V. 14. P. 1328.

23. *Jungmann C. R. et al.* // Nucl. Phys. A. 1982. V. 386. P. 287.

24. *Fowler J. L., Campbell E. C.* // Phys. Rev. 1962. V. 127. P. 2192.

25. *Horen D. J., Harvey J. A., Hill N. W.* // Phys. Rev. C. 1979. V. 20. P. 478; 1981. V. 24. P. 1961.